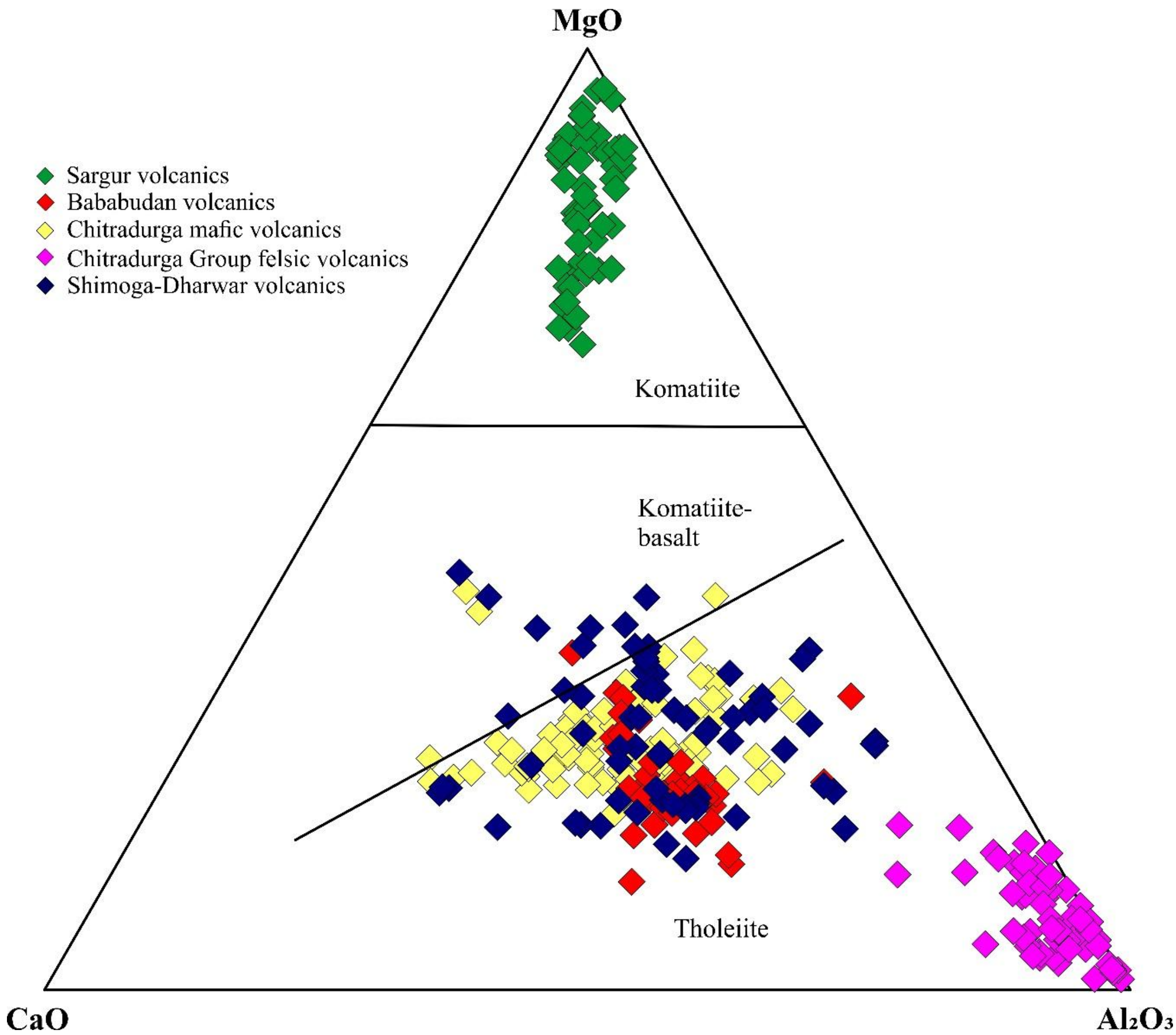

Supplementary figure S1

CaO-MgO-Al_2O_3 ternary plot (after Viljoen et al., 1982) showing dominant komatiite of Sargur and Dharwar Supergroup showing minor komatiitic basalt to majority tholeiite in composition

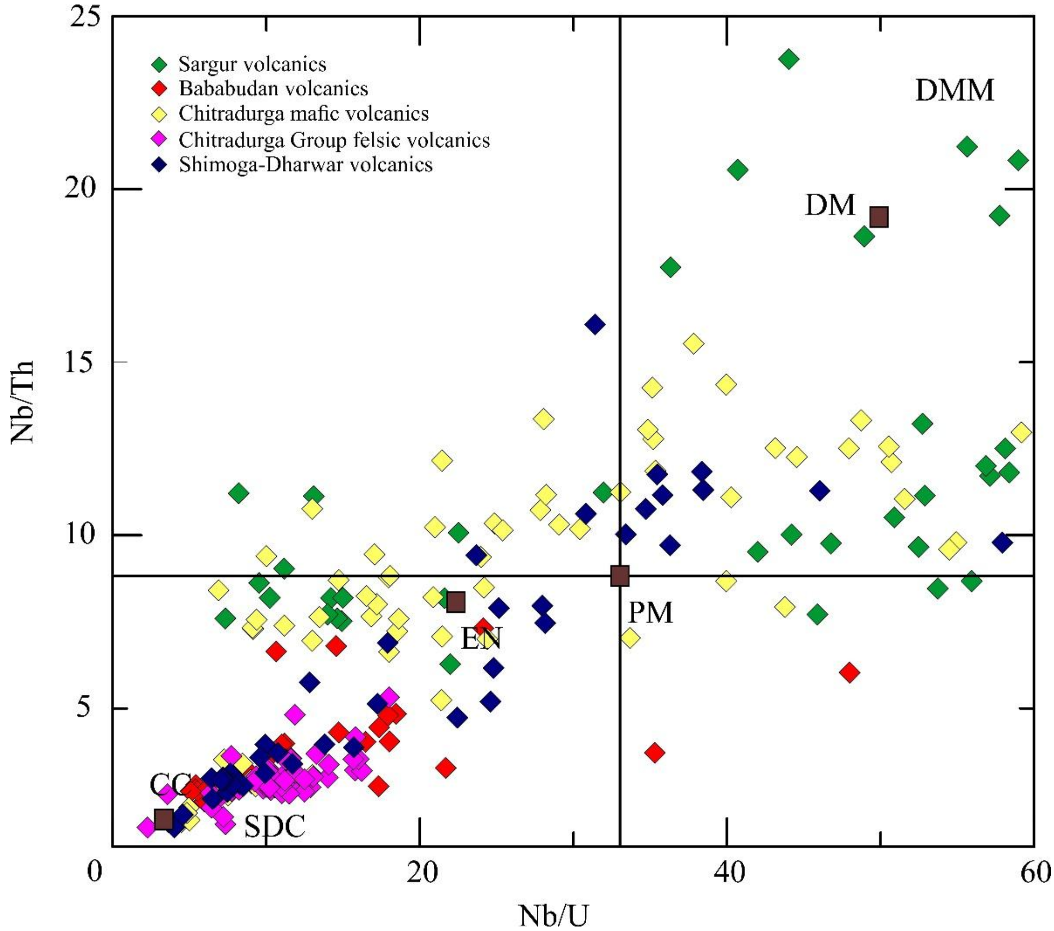

Supplementary figure S2

Nb/U versus Nb/Th (after Saunders et al., 1988) indicating depleted to primitive mantle source for the Sargur and Dharwar Supergroup volcanics with minor crustal contamination and Chitradurga Group felsic volcanics indication dominantly continental crust (CC) contamination. (CC: Continental Crust; SDC: Subduction zone component; EN: Enriched Mantle; PM: Primitive Mantle; DM: Depleted Mantle; DMM: Deep Depleted Mantle)

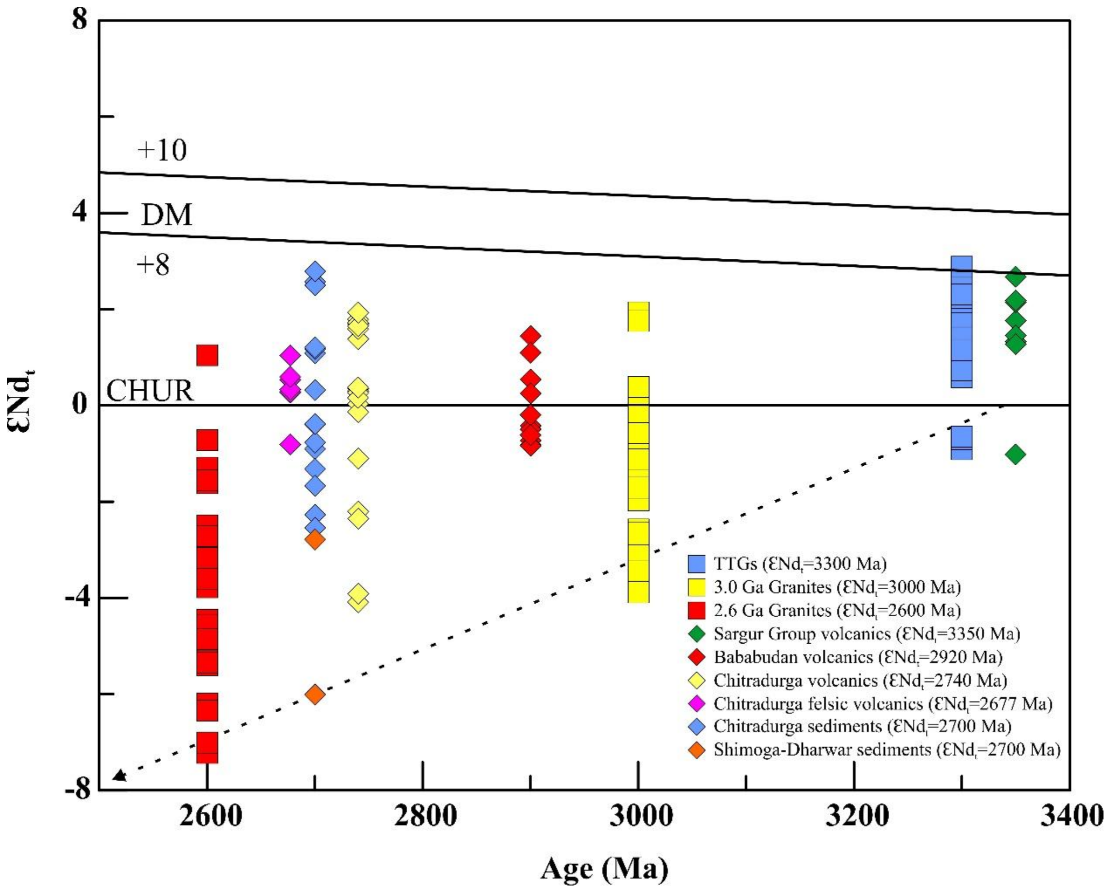

Supplementary figure S3

εNd_t versus time evolution diagram showing the depleted to pre-existing crustal contamination of WDC rock types. In the legend εNd calculated respected to each rock type has been mentioned.

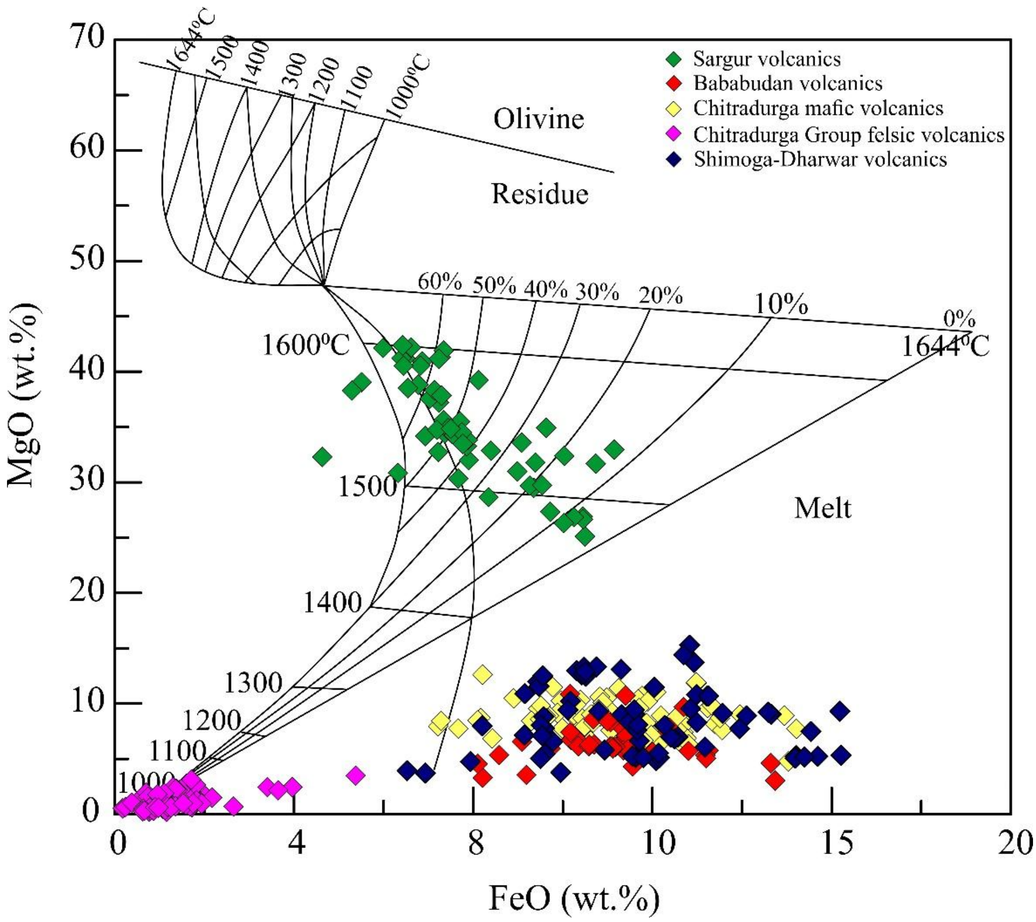

Supplementary figure S4

MgO versus FeO (after Hanson & Langmuir, 1978) showing the volcanic rocks having melt equilibrium with mantle and liquid field. The ca. 3400-3200 Ma komatiite magmas generated at high temperature (1500-1600°C) by high degree (40-50%) melting of deeper mantle and are in equilibrium with the peridotitic mantle until they acquire ultramafic composition. In contrast the younger ca. 3000-2700 Ma mafic volcanics originated by lower degree (20-30%) of shallower mantle at lower temperature (1300-1200°C) whilst the felsic volcanics generated at melting of lower levels of arc crust at ~1000°C.

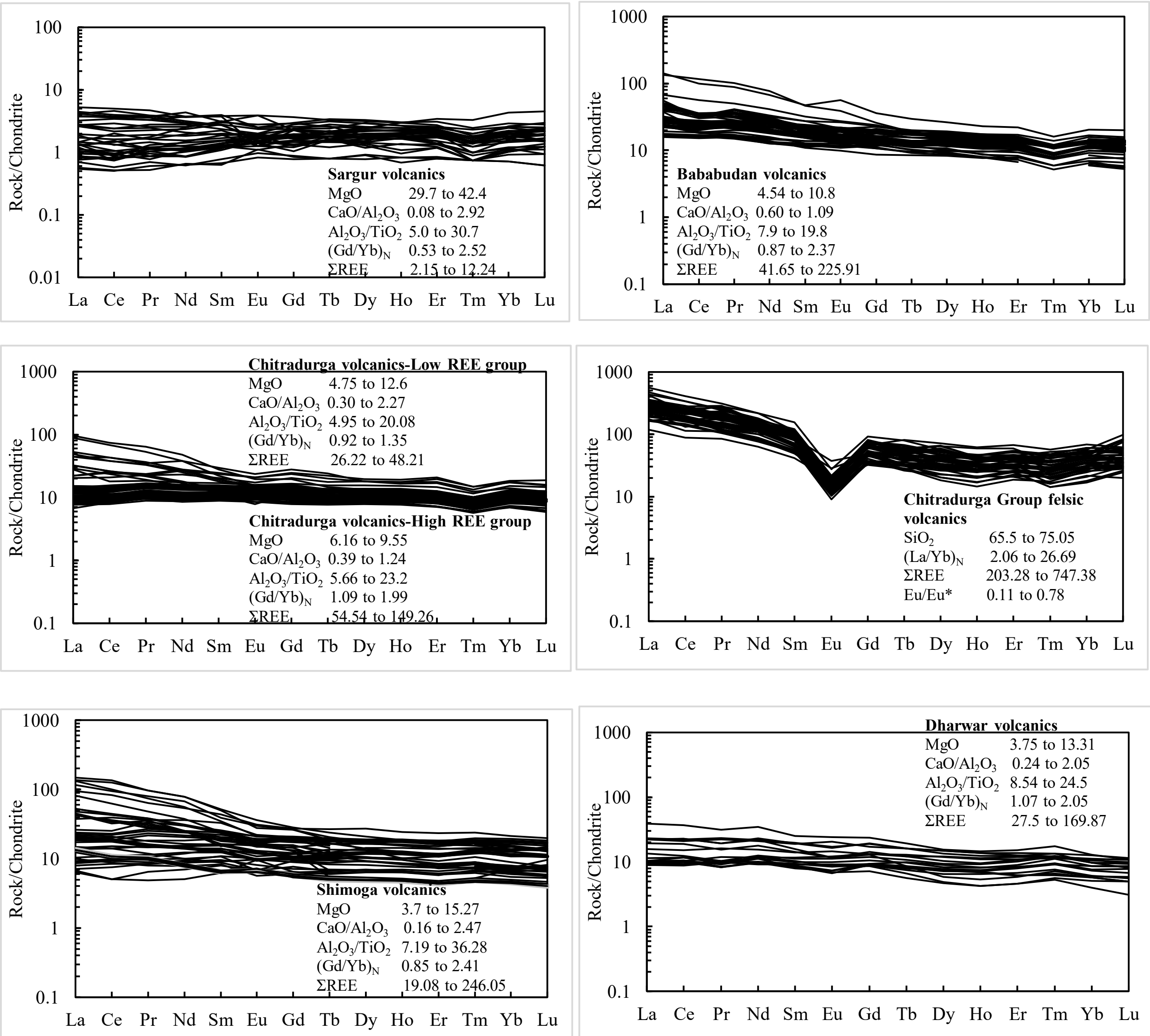

Supplementary figure S5

Chondrite normalized REE patterns of Sargur Group and Dharwar Supergroup (Bababudan, Chitradurga, Shimoga and Dharwar greenstone belt).

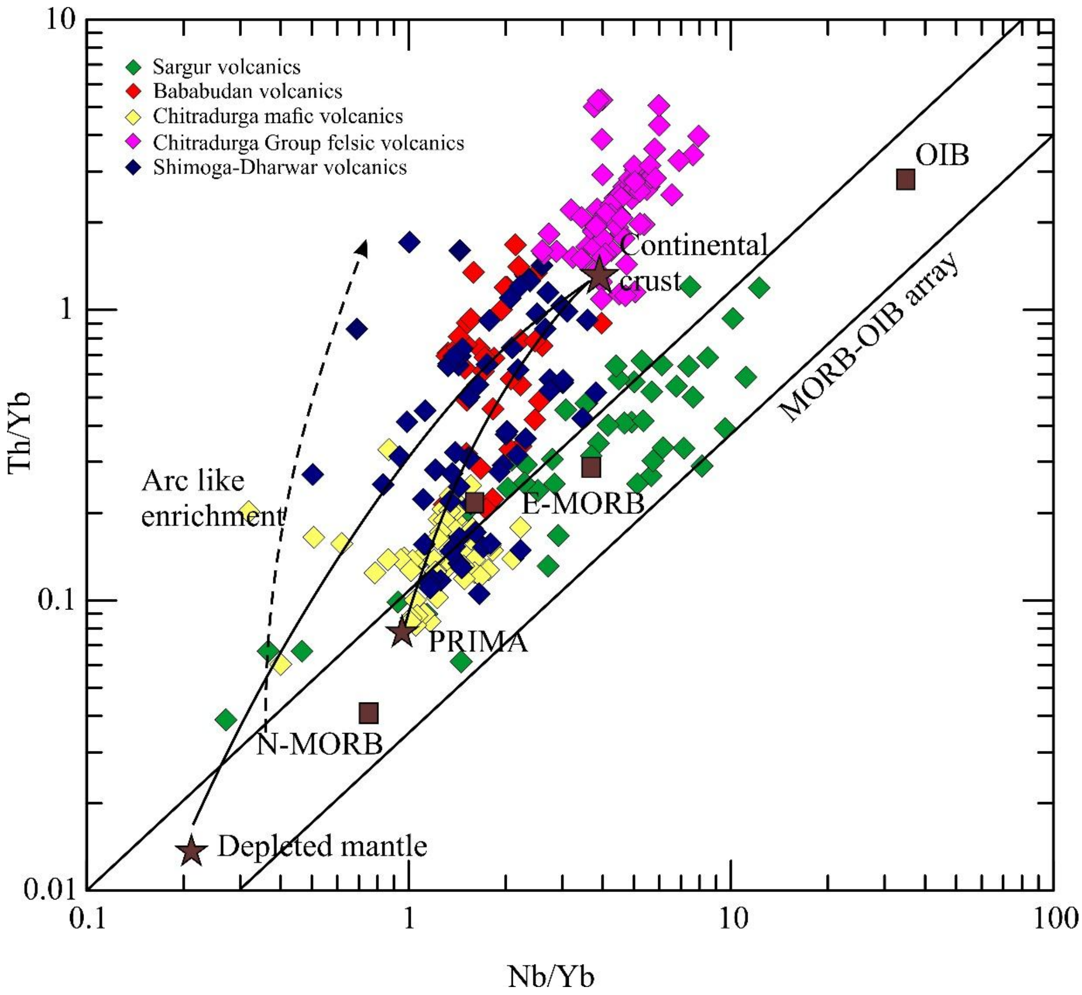

Supplementary figure S6

Nb/Yb versus Th/Yb (after Pearce, 2008) indicating the primitive to depleted mantle source for the Sargur Group of rocks and primitive to arc-like enrichment for the Dharwar Supergroup rocks.

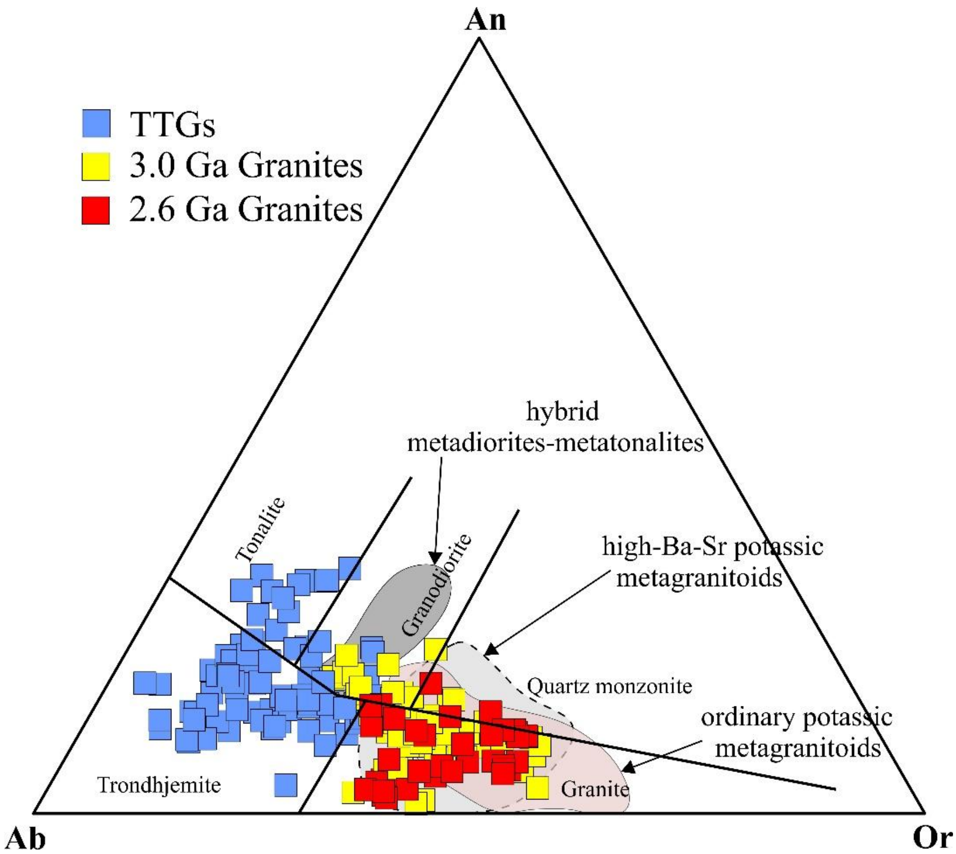

Supplementary figure S7

Normative Ab-An-Or triangular diagram (O'Connors, 1965 fields after Barker, 1979) showing granitoids (TTGs) plot in trondhjemite, tonalite and 3.0 Ga potassic granite, few extending into granodiorite and 2.6 Ga potassic granite dominantly falling in granite field.

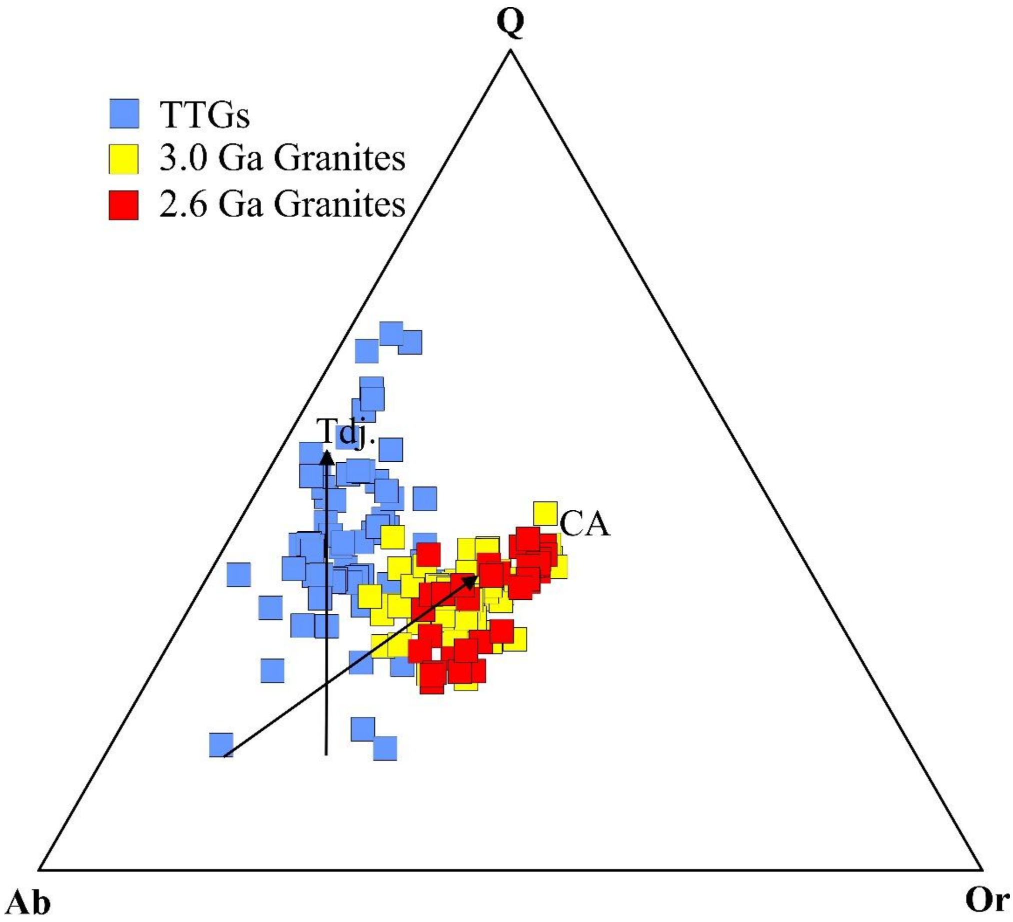

Supplementary figure S8

Normative Q–Ab–Or (O’Connors, 1965 fields after Barker & Arth, 1976) showing the granitoids (TTGs) define trondhjemite and 3.0 Ga, 2.6 Ga potassic granite show calc-alkaline trend (CA).

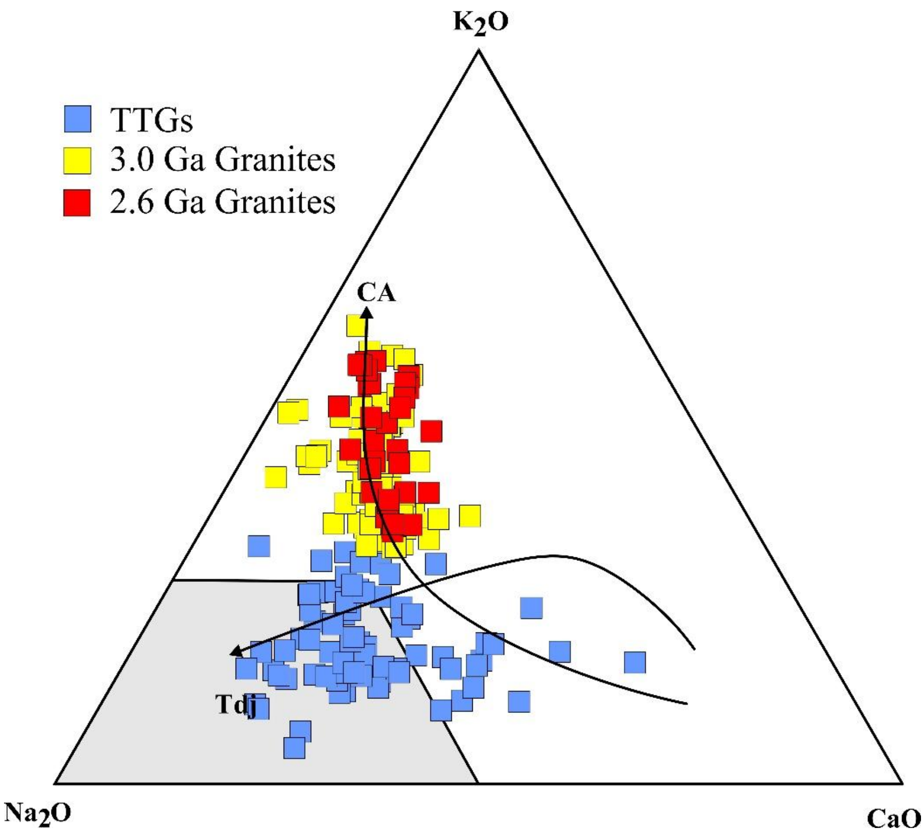

Supplementary figure S9

Na_2O-K_2O-CaO triangular plot (Barker & Arth, 1976) discriminating the calc-alkaline differentiation trend of 3.0 Ga, 2.6 Ga potassic granite from the trondhjemite trend of the TTGs.

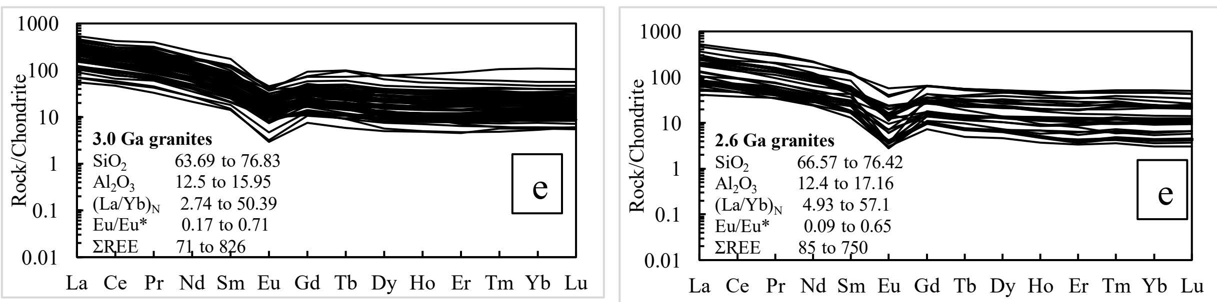

Supplementary figure S10

Chondrite normalized REE patterns of the TTGs, 3.0 Ga and 2.6 Ga potassic granites.

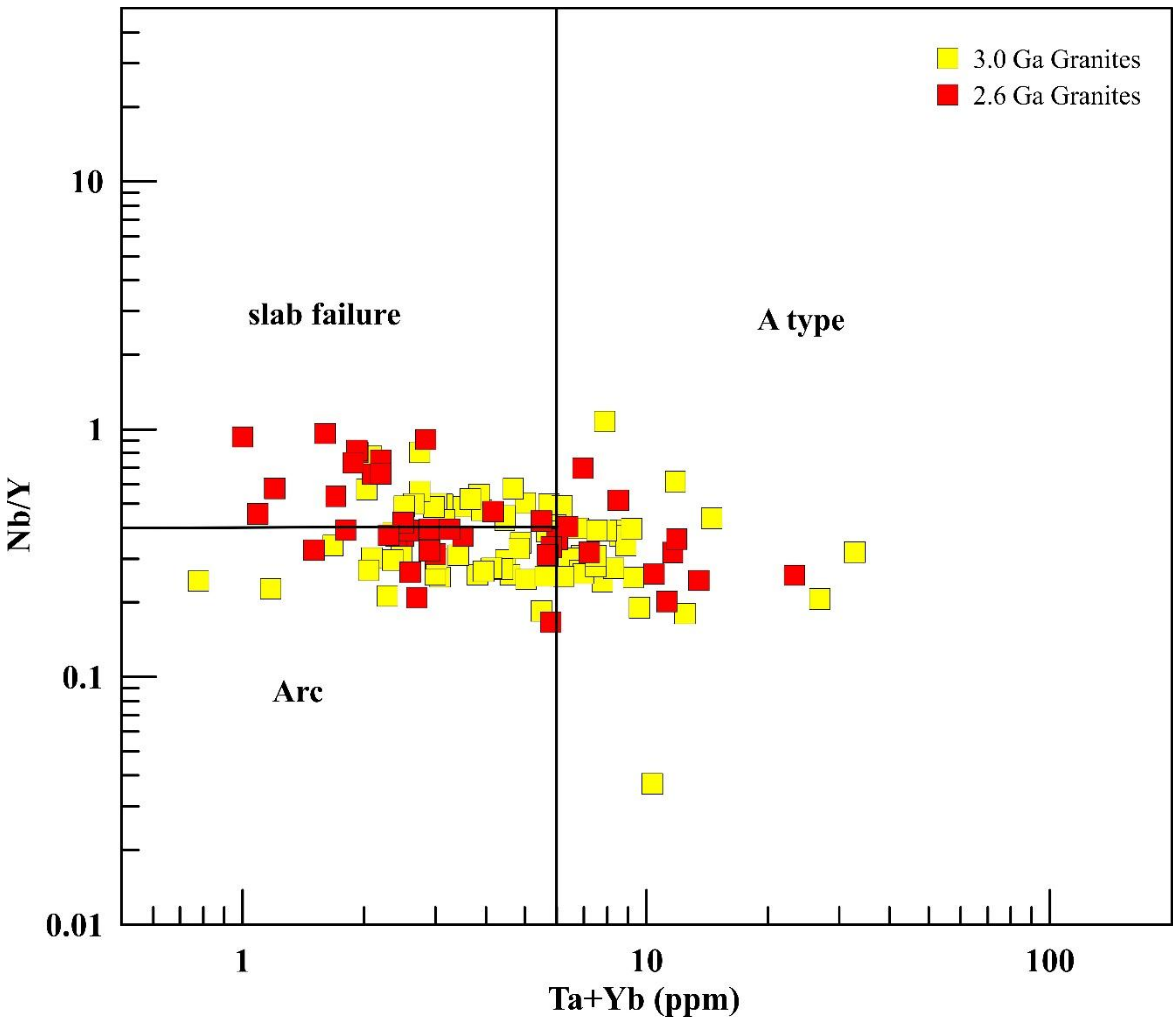

Supplementary figure S11

Nb/Y versus (Ta+Yb) (after Whelen and Hildebrand, 2019) indicating the A-type granite characteristic with some are extending into slab-failure field for the potassic granites from western Dharwar.

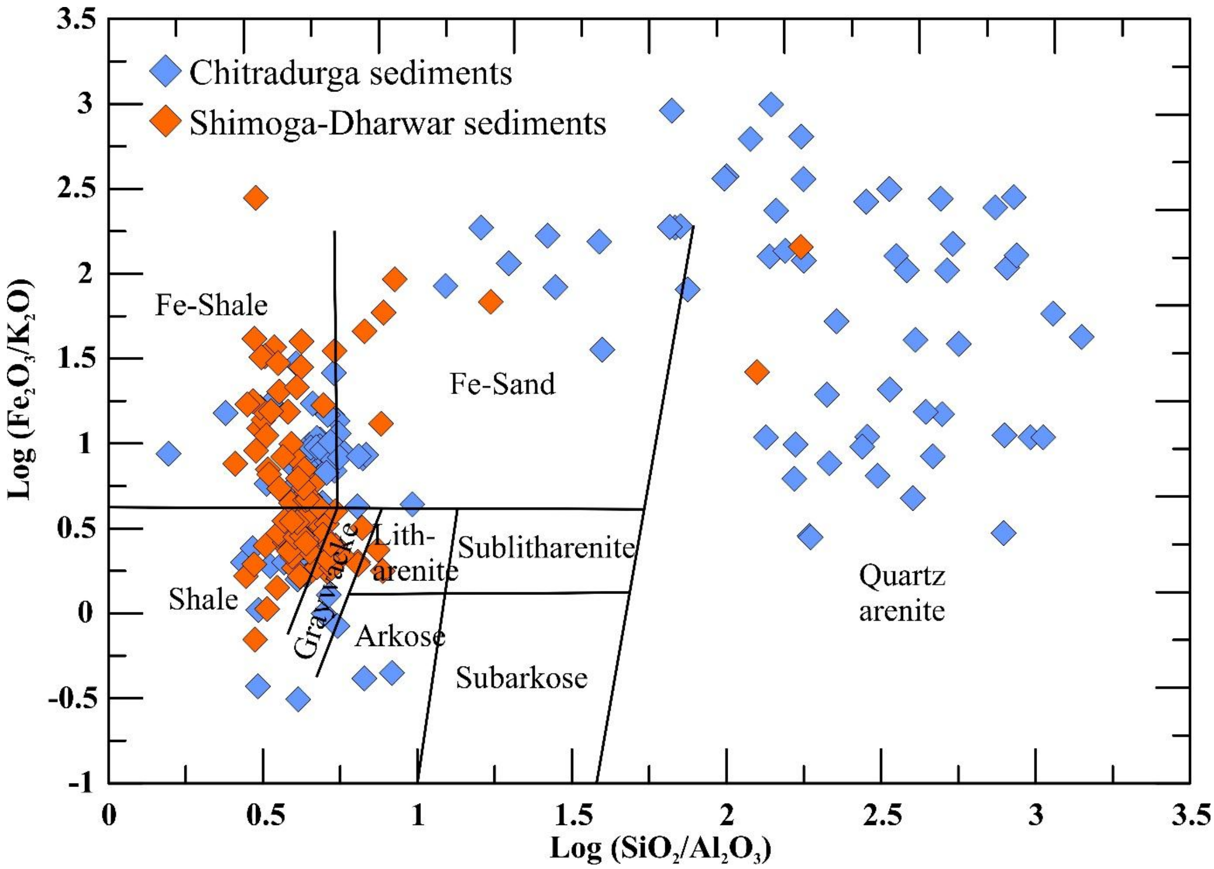

Supplementary figure S12

Binary plot of log (SiO_2/Al_2O_3) versus log (Fe_2O_3/K_2O) (Herron, 1988) the sediments from Chitradurga basin, Shimoga-Dharwar basin fall in the shale, greywacke, lith-arenites to qtz-arenite fields.

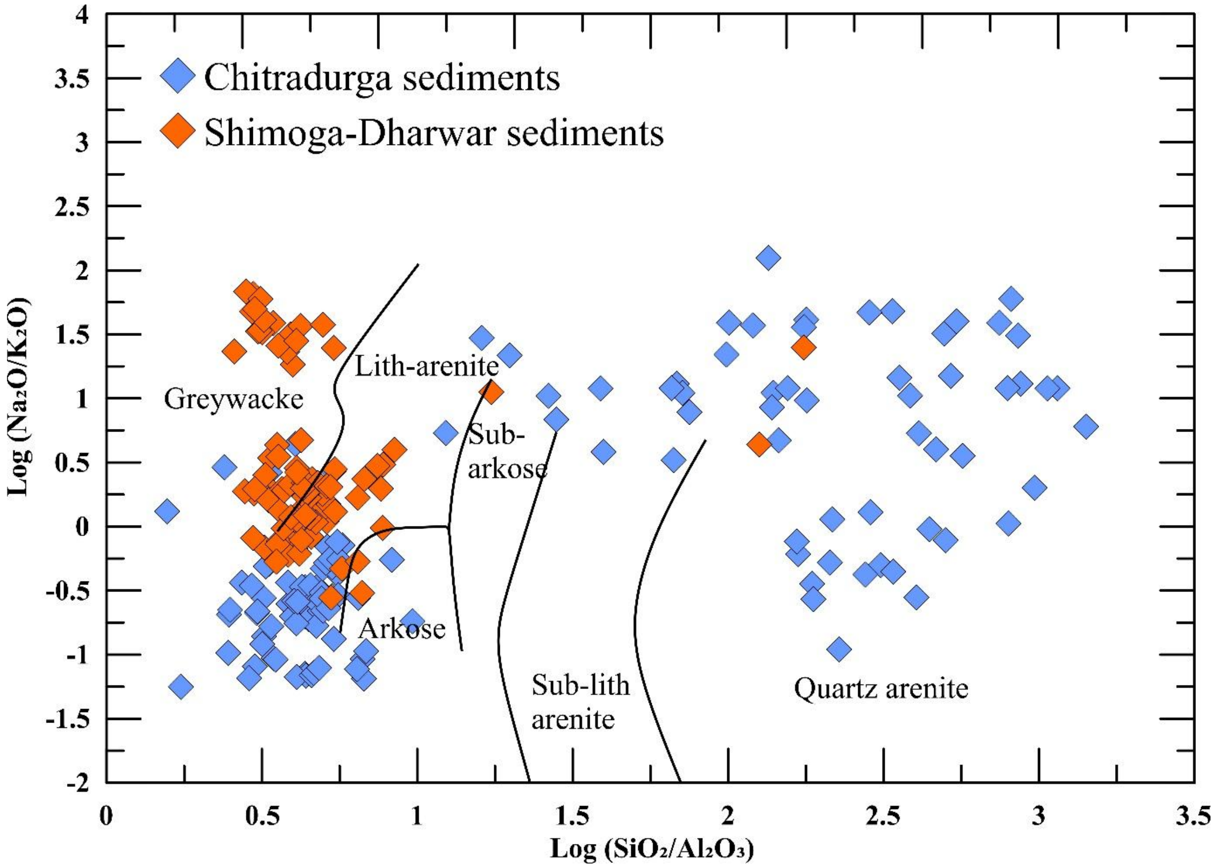

Supplementary figure S13

Plot of log (Na_2O/K_2O) versus log (SiO_2/Al_2O_3) (Pettijohn et al., 1987) where the shales, carbonaceous shale, argillite form a cluster and greywacke from Dharwar region fall on the greywacke field, the arenites from Chitradurga basin falls from lith-arenite to qtz-arenite with few extending into arkose field.

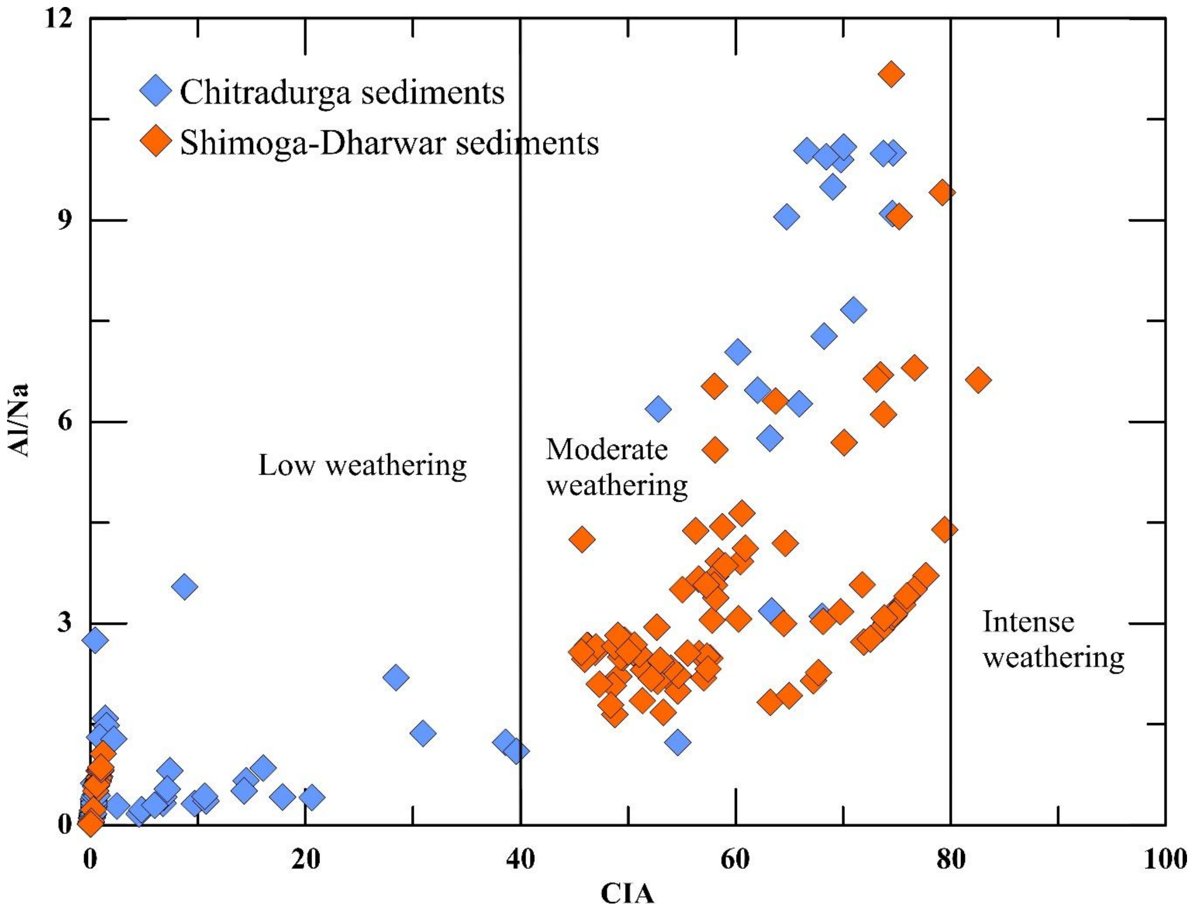

Supplementary figure S14

Chemical index of alteration (CIA) versus Al/Na binary plot (after Harshita et al., 2024) depicts the low to moderate weathering conditions of Chitradurga, Shimoga-Dharwar sediments.

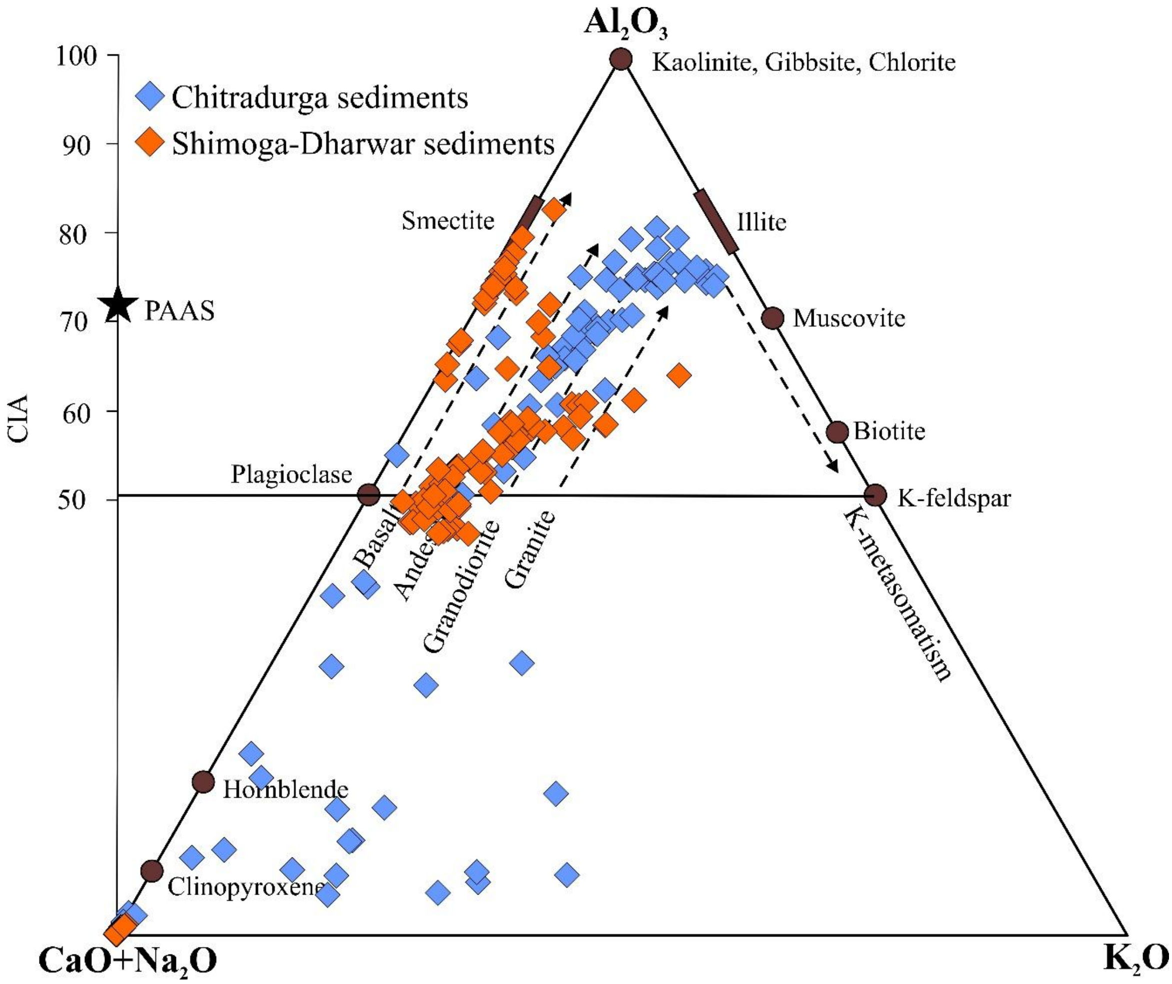

Supplementary figure S15

A-CN-K (A = Al_2O_3, CN = CaO* + Na_2O, K = K_2O) ternary diagram (Nesbitt & Young, 1984) depicting the weathering trend from the granitoid and basaltic source rocks towards the illite field without following K-metasomatic trend.

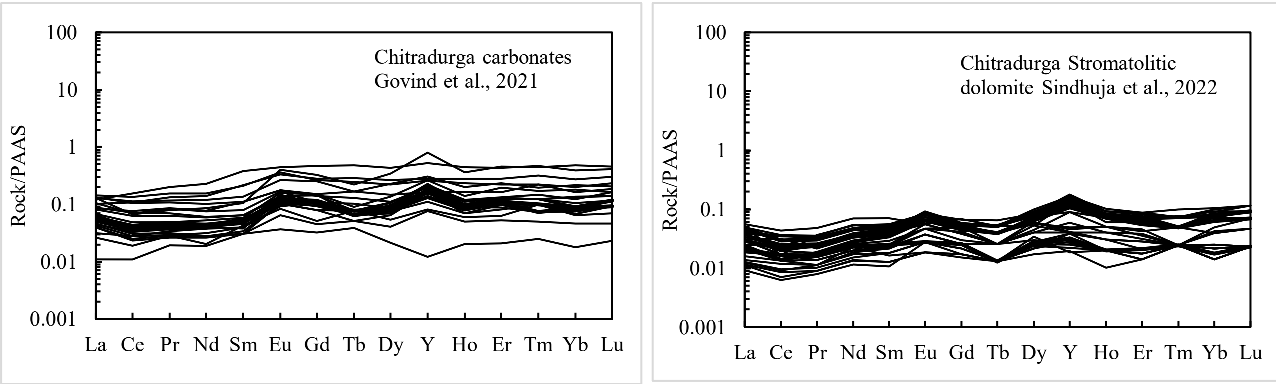

Supplementary figure S16

Post Archean Australian Shale (PAAS) normalized REY patterns of stromatolitic dolomite and carbonates from Chitradurga and Shimoga-Dharwar region. Normalization values after (McLennan et al., 1993)

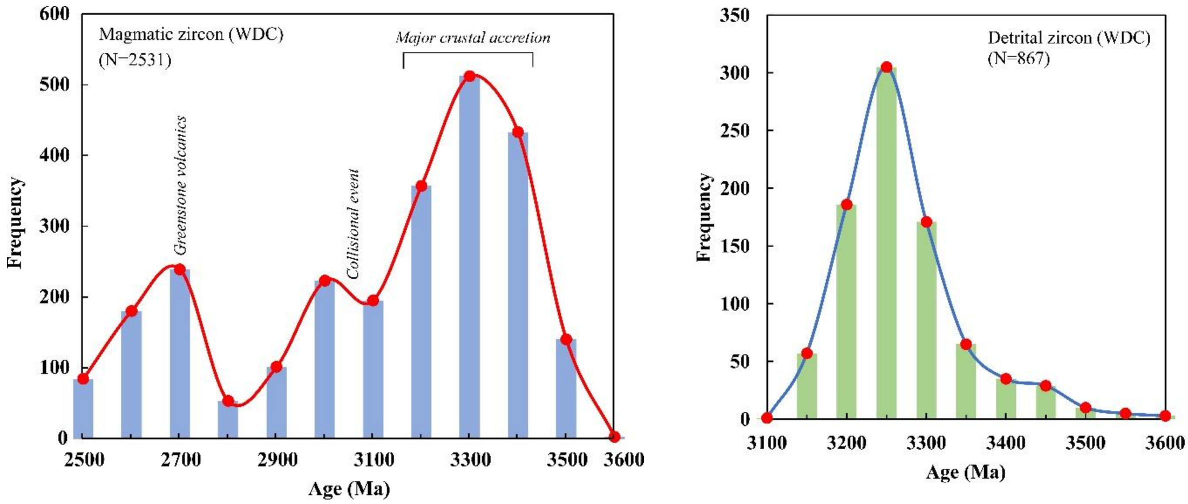

Supplementary figure S17

(a) Histogram diagram of magmatic zircons from western Dharwar craton (data source from Nutman et al., 1996; Jayananda et al., 2006, 2015, 2019, 2023 and reference therein; Guitreau et al., 2017; Han et al., 2019; Manikyamba et al., 2021; Ravindran et al., 2023; Mohan et al., 2023; Wang et al., 2023). (b) Histogram diagram of detrital zircons from western Dharwar craton (data source from Krapez et al., 2020; Khelen et al., 2020; Mitra et al., 2023; Harshita et al., 2024 and references therein).

References

Barker, F., 1979. Trondhjemite: definition, environment and hypothesis of origin. In: Barker F (ed) Trondhjemites, dacites and related rocks. Elsevier, Amsterdam, pp 1–12

Barker, F., Arth, J.G., 1976. Generation of trondhjemite-tonalite liquids and Archean bimodal trondhjemite-basalt suites. Geology 4:596–600

Condie, K.C., 2003. Incompatible element ratios in oceanic basalts and komatiites: tracking deep mantle sources and continental growth rates with time. Geochemistry Geophysics. Geosystems. 4 (1), 1005. https://doi.org/10.1029/2002GC000333.

Defant, M.J., Drummond, M.S., 1990. Derivation of some modern arc magmas by melting of young subducted lithosphere. Nature 347, 662–665.

Guitreau, M., Mukasa, S. B., Loudin, L., & Krishnan, S. 2017. New constraints on the early formation of the Western Dharwar Craton (India) from igneous zircon U-Pb and Lu-Hf isotopes. Precambrian Research, 302, 33-49. https://doi.org/10.1016/j.precamres.2017.09.016

Han, Y.S., Santosh, M., Ganguly, S., Li, S.S., 2019. Evolution of a Mesoarchean suprasubduction zone mantle wedge in the Dharwar craton, southern India: Evidence from petrology, geochemistry, zircon U-Pb geochronology, and Lu-Hf isotopes. Geological Journal, 1-22. DOI: 10.1002/gj.3440

Hanson, G.N., Langmuir, C.H., 1978. Modelling of major elements in mantle-melt systems using trace element approaches. Geochimica et Cosmochimica Acta, 42, 725–741. https://doi.org/10.1016/0016-7037(78)90090-X

Harshitha, G., Manikyamba, C., Santosh, M., Yang, C.-X., Krishna, A.K., Sai, V.V.S., Reddy, I.P., 2024. Paleo-Mesoarchean sedimentary record in the Dharwar Craton, India: implications for Archean Ocean oxygenation. Geoscience Frontiers, 15, 101701. https://doi.org/10.1016/j.gsf.2023.101701

Herron, M.M., 1988. Geochemical classification of terrigenous sands and shales from core or log data. Journal of Sedimentary Petrology, 58, 820–829

Jahn, B., Glikson, A.Y., Peucat, J.-J., Hickman, A.H., 1981. REE geochemistry and isotopic data of Archean silicic volcanics and granitoids from the Pilbara block, Western Australia: implications for early crustal evolution. Geochimica et Cosmochimica Acta, 45, 1633–1652.

Jayananda, M., Chardon, D., Peucat, J.J., Capdevila, R., 2006. 2.61Ga potassic granites and crustal reworking in the western Dharwar Craton, southern India: Tectonic, geochronologic and geochemical constraints. Precambrian Research, 150, 1–26.

Jayananda, M., Chardon, D., Peucat, J. J., Fanning, C. M., 2015. Paleo-to Mesoarchean TTG accretion and continental growth in the western Dharwar craton, Southern India: constraints from SHRIMP U–Pb zircon geochronology, whole-rock geochemistry and Nd–Sr isotopes. Precambrian Research, 268, 295-322. https://doi.org/10.1016/j.precamres.2015.07.015

Jayananda, M., Guitreau, M., Aadhiseshan, K. R., Miyazaki, T., & Chung, S. L. 2023. Origin of the oldest (3600–3200 Ma) cratonic core in the Western Dharwar Craton, Southern India: Implications for evolving tectonics of the Archean Earth. Earth-Science Reviews, 236, 104278. https://doi.org/10.1016/j.earscirev.2022.104278

Jayananda, M., Martin, G., Tarun Thomas, T., Martin, H., Aadhiseshan, K.R., Gireesh, R. V., Peucat, J.-J., Satyanarayanan, M., 2019. Geochronology and geochemistry of Meso- to Neoarchean magmatic epidote-bearing potassic granites, Western Dharwar Craton (Bellur–Nagamangala–Pandavpura corridor), Southern India: implications for the successive stages of crustal reworking and cratonization. In: Dey, S., Moyen, J.-F. (Eds.), Archean Granitoids of India: Windows into Early Earth Tectonics. Geological Society, London, Special Publications, vol 489. Geological Society of London, London. https://doi.org/10.1144/SP489-2018-125

Jensen, L.S., 1976. A new method of classifying alkali volcanic rocks: Ontario Division Mineral. Miscellaneous Paper 66, 22.

Khelen, A.C., Manikyamba, C., Tang, L., Santosh, M., Subramanyam, K.S.V., Singh, T.D., 2020. Detrital zircon U-Pb geochronology of stromatolitic carbonates from the greenstone belts of Dharwar Craton and Cuddapah basin of Peninsular India. Geoscience Frontiers, 11, 229–242. https://doi.org/10.1016/j.gsf.2019.04.010

Krapez, B., Srinivasa Sarma, D., Ram Mohan, M., McNaughton, N.J., Rasmussen, B., Wilde, S.A., 2020. Tectonostratigraphy of the Late Archean Dharwar Supergroup, Dharwar Craton, India: Defining a tectonic history from spatially linked but temporally distinct intracontinental and arc-related basins. Earth-Science Rev. 201, 102966 https://doi.org/10.1016/j.earscirev.2019.102966

Manikyamba, C., Ganguly, S., Santosh, M., Tang, L., Sindhuja, C.S., Pahari, A., Singh, T. D., Saha, A., 2021. Tectonic juxtaposition of plume and subduction derived magmatic sequences in the Bababudan greenstone terrane, western Dharwar Craton, India: Constraining crustal accretion processes in a Neoarchean subduction-collision orogeny. Precambr. Res. 355, 106097. https://doi.org/10.1016/j.precamres.2021.106097

McLennan, S.M., Hemming, S., McDaniel, D.K., Hanson, G.N., 1993. Geochemical approaches to sedimentation, provenance, and tectonics. In: Processes Controlling the

Mitra, A., Dey, S., Das, P., Zong, K., & Liu, Y. 2023. Nucleation and growth of western Dharwar Craton: A Paleoarchean to Mesoarchean evolutionary history recorded in sediment geochemistry and detrital zircon U-Pb-Hf isotopes-trace elements. Lithos, 448-449, 107148. https://doi.org/10.1016/j.lithos.2023.107148

Mohan, M. R., McNaughton, N. J., Sarma, D. S., Rajamanickam, M., Fletcher, I. R., Wilde, S. A. & Balakrishnan, S. 2023. Petrogenesis of Meso-Neoarchean granitoids from the Chitradurga Greenstone Belt: Implications on crustal growth and reworking of the Dharwar Craton, southern India. Journal of Asian Earth Sciences, 242, 105494. https://doi.org/10.1016/j.jseaes.2022.105494

Mukherjee, R., Mondal, S.K., Frei, R., Rosing, M.T., Waight, T.E., Zhong, H., Kumar, G.R., 2012. The 3.1 Ga Nuggihalli chromite deposits, Western Dharwar craton (India): geochemical and isotopic constraints on mantle sources, crustal evolution and implications for supercontinent formation and ore mineralization. Lithos 155392–155409.

Nesbitt, H.W., and Young, G.M., 1984. Prediction of some weathering trends of plutonic and volcanic rocks based on thermodynamic and kinetic considerations. Geochimica et Cosmochimica Acta, 48, 1523–1534.

Nutman, A.P., Chadwick, B., Krishna Rao, B., Vasudev, V.N., 1996. SHRIMP U/Pb zircon ages of acid volcanic rocks in the Chitradurga and Sandur groups, and granites adjacent to the Sandur schist belt, Karnataka. J. Geol. Soc. India 47, 153–164. https://doi.org/10.17491/jgsi/1996/470202

O'Connor, J.T., 1965. A classification for quartz-rich igneous rocks based on feldspar ratios. US Geological Survey, 525(B):79–84

Pearce, J.A., 2008. Geochemical fingerprinting of oceanic basalts with applications to ophiolite classification and the search for Archean oceanic crust. Lithos 100, 14–48.

Pettijohn, F.J., Potter, P.E., Siever, R., 1987. Sand and Sandstone. Springer-Verlag, New York, p. 553

Ravindran, A., Mezger, K., Balakrishnan, S., Berndt, J., Ranjan, S., Upadhyay, D., 2023. Formation of Paleo- to Meso-Archean continental crust in the western Dharwar Craton, India: Constraints from U-Pb zircon ages and Hf-Pb-Sr isotopes of granitoids and sedimentary rocks. Chem. Geol. 615, 121196. https://doi.org/10.1016/j.chemgeo.2022.121196

Saunders, A.D., Norry, M.J., and Tarney, J., 1988. Origin of MORB and chemically-depleted mantle reservoirs: Trace element constrains, in Menzies, M.A., and Cox, K.G., eds., Oceanic and continental lithosphere: Similarities and differences: London, Oxford university press, 415–445.

Viljoen, M.J., Viljoen, F.P., Pearton, T.N., 1982. The nature and distribution of Archaean komatiite volcanics in South Africa. In: Arndt, N.T., Nisbet, E.G. (Eds.), Komatiites. Allen and Unwin, London, pp. 53–79.

Wang, M. X., Santosh, M., Jayananda, M., Yang, C-X., Thomas, Tarun T., Kim, Sung Won., 2023. Trondhjemites from the Western Dharwar Craton, Southern India: Implications for Mesoarchean crustal growth. Lithos, 462–463, 107410. https://doi.org/10.1016 /j.lithos.2023.107410

Whalen, J., and Hildebrand, R., 2019. Trace element discrimination of arc, slab failure, and A-type granitic rocks, Lithos, 348-349, 105179. https://doi.org/10.1016/j.lithos.2019.105179